

# A Renormalization Scheme and Skewness of Height Fluctuations in $(1 + 1)$ -dimensional VLDS Dynamics

Tapas Singha & Malay K. Nandy

Department of Physics, Indian Institute of Technology Guwahati, Guwahati 781039, India.

E-mail: s.tapas@iitg.ernet.in & mknandy@iitg.ernet.in

**Abstract.** We study the  $(1 + 1)$ -dimensional Villain, Lai, and Das Sarma (VLDS) equation driven by a Gaussian white noise and implement a renormalization scheme without rescaling at one-loop order. Using a diagrammatic method, we calculate the renormalized second and third moments in the large-scale and long-time limits. The ensuing skewness value is  $S = -0.0441$ . This (negative) value is consistent with the numerical prediction of Das Sarma *et al.* [Phys. Rev. E **53** 359 (1996)].

PACS Nos. 81.15.Aa, 68.35.Fx, 64.60.Ht, 05.10.Cc

**Keywords:** Kinetic roughening (Theory), Self-affine roughness (Theory), Dynamical processes (Theory), Stochastic processes (Theory).

## 1. Introduction

In the last few decades, one of the most widespread, useful and fascinating topics of research in nonequilibrium statistical physics is kinetic interface roughening [1, 2, 3, 4, 5, 6, 7]. A great deal of experiments and numerical simulations have been carried out in this field and a few analytical methods have been employed including the renormalization group (RG) to understand the scaling behavior, exponents and thereby universality of a growing surface. A linear continuum dynamics of surface growth is described by the Edwards-Wilkinson [8] (EW) equation where the surface profile evolves due to random deposition and surface tension.

A nonlinear paradigmatic equation for surface growth, as proposed by Kardar, Parisi and Zhang (KPZ) [9, 10], describes a wide range of surface growth phenomena such as the eden model [11], ballistic deposition [12], restricted solid-on-solid model (RSOS), all belonging to a common universality class as they exhibit the same scaling exponents.

The growth of a thin film using the molecular beam epitaxy (MBE) is dominated by surface diffusion [13] at high temperatures, where atomic evaporation [14], desorption, bulk defects [15], hangs and overhangs are negligibly small. In MBE, atoms are deposited one-by-one for the preparation of high quality thin films [16]. On the other hand, at low

temperatures, a growing surface would be amorphous instead of crystalline [17] because deposited particles would not have much energy to overcome the height barriers so that they can settle down at the lowest energy positions. According to Mullins's theory [18] such surface growth obeys the equation of continuity

$$\frac{\partial h}{\partial t} = -\nabla \cdot \mathbf{j} \quad (1)$$

where the particle current is  $\mathbf{j} = \nabla \mu(\mathbf{x}, t)$  and local chemical potential  $\mu(\mathbf{x}, t)$  is related to the surface curvature as  $\mu(\mathbf{x}, t) = \kappa \nabla^2 h(\mathbf{x}, t)$ . Fourier transforming and rescaling of equation 1 yield roughness, dynamic and growth exponents as  $\chi = (4 - d)/2$ ,  $z = 4$  and  $\beta = (4 - d)/8$  respectively,  $d$  being the substrate dimension. Wolf and Villain [19] (WV) studied a model with random deposition and surface diffusion in one dimension, where the particles are relaxed to the minimum energy positions yielding roughness and dynamic exponents,  $\chi = 1.4 \pm 0.1$  and  $z = 3.8 \pm 0.5$ , that indicates a different universality class from those of EW and KPZ. These exponents are close to those obtained from equation 1. Das Sarma and Tamborenea (DT) [20] investigated a deposition model with surface relaxation and estimated roughness and growth exponents as  $\chi \approx 1.5$  and  $\beta = 0.375 \pm 0.005$  in one spatial dimension. Krug [21] studied the height-height correlation function and structure factor in one dimension by taking the solid-on-solid (SOS) model with DT [20] relaxation rule where overhangs are not present. His obtained growth exponent is  $\beta = 0.37 \pm 0.01$ , satisfying the scaling relation of equation 1. The step size distribution of his study yields a non zero skewness in one substrate dimension. This implies that the distribution of height fluctuations is not Gaussian unlike that of equation 1 and consequently suggesting that the continuum model for the MBE growth process must be a nonlinear dynamical equation.

Sun, Guo and Grant (SGG) [22] proposed a nonlinear equation for surface growth where total volume under the interface is conserved, including noise conservation. They obtained a distinct set of exponents given by  $\chi = \frac{2-d}{3}$  and  $z = \frac{10+d}{3}$  that agree with the conserved restricted solid on solid (CRSOS) model for  $d = 1$ .

Considering a geometrical interpretation, Villain, Lai and Das Sarma (VLDS) [17, 23] proposed a nonlinear equation with non-conserved noise for the MBE process. This dynamical equation is known as the VLDS equation, written as

$$\frac{\partial h}{\partial t} = -\nu_0 \nabla^4 h + \frac{\lambda_0}{2} \nabla^2 (\nabla h)^2 + \eta, \quad (2)$$

where  $h(\mathbf{x}, t)$  is the height of the fluctuating surface at position  $\mathbf{x}$  and time  $t$ ,  $\nu_0$  is the diffusion constant and  $\eta(\mathbf{x}, t)$  is a Gaussian white noise with zero mean and covariance

$$\langle \eta(\mathbf{x}, t) \eta(\mathbf{x}', t') \rangle = 2D_0 \delta^d(\mathbf{x} - \mathbf{x}') \delta(t - t'). \quad (3)$$

where  $D_0$  is a constant.

Family and Vicsek [5] proposed the dynamic scaling for the surface width (standard deviation) as

$$w(L, t) \sim L^\chi F\left(\frac{t}{L^z}\right). \quad (4)$$

For large  $\tau$ ,  $F(\tau) = \text{Const.}$  and for small  $\tau$ ,  $F(\tau) \sim \tau^\beta$ . The ratio  $\beta = \frac{\chi}{z}$  is called the growth exponent.

Through one-loop dynamic RG calculations [23], Lai and Das Sarma as well as Tang and Nattermann [24] independently obtained the roughness, dynamic and growth exponents as  $\chi = \frac{4-d}{3}$ ,  $z = \frac{8+d}{3}$  and  $\beta = \frac{4-d}{8+d}$ . Janssen argued in the Ref.[25] that KPZ like Galilean transformation in SGG and VLDS equations are mathematically ill defined and thereby the exponents following from an RG calculations are to be corrected. Accounting for two-loop corrections in an RG calculation, he obtained small corrections to the exponents in each dimensions. Subsequently, numerical works [26, 27] were devoted to capture corrections to the exponents. These numerical corrections turned out to be larger than Janssen's corrections. However, no conclusions could be reached regarding the role of vertex corrections in their numerical simulations. Katzav [28] investigated equation 2 via a self-consistent-expansion method which has close relation to mode-coupling approach and obtained the same set of exponents as the one-loop dynamic RG results. It may however be noted that Katzav's self-consistent integral equations were equivalent to a renormalized perturbation theory at one-loop order without vertex renormalization.

There exist two types of investigations in the literature. One of them is finding the scaling exponents through different growth models and comparing them with the calculated exponents corresponding to the continuum equations. The other type of work is the derivation of a continuum equation from the discrete model using the principle of symmetry or re-parametrization of invariance [29] (alternatively using the master equation [30, 31, 32, 33]). Wilby *et al.* [34] studied the SOS model by using Monte-Carlo-Simulation and estimated the growth exponents  $\beta = 0.333 \pm 0.010$  in  $d = 1$  dimension which agrees with the dynamic RG result. A conserved growth model with RSOS condition, in  $1 + 1$  dimensions, has been studied by Kim and Kim in the Refs. [35, 36] and their estimated exponents (roughness and growth exponents  $\chi = 0.95 \pm 0.04$  and  $\beta = 0.32 \pm 0.01$  respectively) agree with the calculated exponents from dynamic RG.

There exist many numerical studies to obtain the scaling exponents which in turn determine the universality classes. A detailed study of the height fluctuations involves the determination of its probability distribution function that determines the universality class of the growth process. However, obtaining the full probability distribution function is an analytically impossible task and alternatively a few lower order moments yielding the skewness and kurtosis could be studied. The  $n$ th moment of the height fluctuations is defined as

$$W_n = \langle [h(\mathbf{x}, t) - \bar{h}(t)]^n \rangle, \quad (5)$$

and the moments follow the power laws at stationary state as,  $W_n \sim L^{n\chi}$ , where  $L$  is the substrate size. Skewness is defined as

$$S = \frac{W_3}{(W_2)^{3/2}}. \quad (6)$$

It may be noted that numerical attempts to obtain the skewness for the VLDS type growth is rather rare. For example, Das Sarma *et al.* [37] considered a discrete LDS model and obtained  $S = -0.1 \pm 0.15$  in the steady state.

However, there appears to be no attempts to obtain the value of skewness via analytical means directly from the VLDS equation. Since skewness is an important property of the probability distribution function, it is indispensable to calculate its value for the height fluctuations governed by the VLDS dynamics so that this fluctuations can be distinguished from those governed by other dynamical processes.

In this paper we calculate the second and third moments of the height fluctuations in the stationary state directly from the VLDS equation starting from flat initial condition employing a diagrammatic methods and a renormalization scheme without rescaling. This allows for the calculation of the skewness given by equation 6.

The rest of the paper is organized in the following way. Section II presents a renormalization group scheme without rescaling. Section III presents the calculation of the second moment  $W_2$ . In Section-IV, we calculate the third moment  $W_3$  and thereby the value of skewness is obtained. Section-V calculates the skewness and Section-VI gives a Discussion and Conclusion.

## 2. Renormalization Scheme Without Rescaling

In this section, we employ an RG scheme without rescaling that was previously used by Yakhot and Orszag [38, 39] in the case of fluid turbulence and, later, it was applied to the stochastic KPZ dynamics [40, 41] We begin with the Fourier transformation of the VLDS equation (equation 2), namely,

$$(-i\omega + \nu_0 k^4)h(\mathbf{k}, \omega) = \eta(\mathbf{k}, \omega) - \frac{\lambda_0}{2} k^2 \int \int \frac{d^d q d\Omega}{[2\pi]^{d+1}} [\mathbf{q} \cdot (\mathbf{k} - \mathbf{q})] h(\mathbf{q}, \Omega) h(\mathbf{k} - \mathbf{q}, \omega - \Omega). \quad (7)$$

We shall use equation 7 to obtain the renormalized surface diffusivity as well as the skewness of the height fluctuations in  $(1 + 1)$ -dimensions.

### 2.1. Scale Elimination

In the Fourier space, we split the height and noise fields into slow and fast modes, namely,  $h^<(\mathbf{k}, \omega)$  and  $h^>(\mathbf{k}, \omega)$ , and  $\eta^<(\mathbf{k}, \omega)$  and  $\eta^>(\mathbf{k}, \omega)$ , where  $h^>(\mathbf{k}, \omega)$  and  $\eta^>(\mathbf{k}, \omega)$  belong to the shell  $\Lambda_0 e^{-r} \leq k \leq \Lambda_0$ . The fluctuating modes  $h^>(\mathbf{k}, \omega)$  are eliminated by means of integration and its effect is accounted for as corrections to the model parameters ( $\nu_0$ ,  $D_0$  and  $\lambda_0$ ). As a consequence, we obtain an equation for the slow modes  $h^<(\mathbf{k}, \omega)$

$$[-i\omega + \nu_0 k^4 + \Sigma(\mathbf{k}, \omega)]h^<(\mathbf{k}, \omega) = \eta^<(\mathbf{k}, \omega) - \left(\frac{\lambda_0}{2}\right) k^2 \int \int \frac{d^d q d\Omega}{[2\pi]^{d+1}} [\mathbf{q} \cdot (\mathbf{k} - \mathbf{q})] h^<(\mathbf{q}, \Omega) h^<(\mathbf{k} - \mathbf{q}, \omega - \Omega), \quad (8)$$

in the momentum space  $0 \leq (k, p, q) \leq \Lambda_0 e^{-r}$ . Here, the self energy correction is given by

$$\begin{aligned} \Sigma(k, \omega) &= 4 \left( \frac{-\lambda_0}{2} \right)^2 (2D_0) k^2 \int^> \frac{d^d q}{[2\pi]^d} [\mathbf{q} \cdot (\mathbf{k} - \mathbf{q})] [\mathbf{k} \cdot (\mathbf{q} - \mathbf{k})] q^2 \\ &\times \int_{-\infty}^{\infty} \frac{d\Omega}{[2\pi]} G_0^>(\hat{q}) |G_0^>(\hat{k} - \hat{q})|^2 \end{aligned} \quad (9)$$

with  $G_0(\hat{k}) \equiv G_0(\mathbf{k}, \omega) = [-i\omega + \nu_0 k^4]^{-1}$  is a bare propagator. Following Ref.[42, 38, 39], we integrate over the internal frequency  $\Omega$  and invoke the transformation  $\mathbf{q} \rightarrow (\mathbf{q} + \mathbf{k}/2)$ . Performing the internal momentum integration in the shell  $\Lambda_0 e^{-r} \leq q \leq \Lambda_0$ , a correction to the surface diffusivity is obtained as

$$\Delta\nu = \frac{\lambda_0^2 D_0}{\nu_0^2} \frac{S_d}{[2\pi]^d} \left( \frac{6-d}{4d} \right) \left[ \frac{e^{(4-d)r} - 1}{(4-d)\Lambda_0^{4-d}} \right] \quad (10)$$

in the large-scale ( $q \gg k$ ) long-time limits ( $\omega \rightarrow 0$ ). Here  $S_d = \frac{2\pi^{d/2}}{\Gamma(d/2)}$  is the area of a sphere of unit radius embedded in a  $d$ -dimensional space and  $\Sigma(\mathbf{k}, 0) = k^4 \Delta\nu$ . Consequently, we obtain an effective diffusivity as

$$\nu^<(r) = \nu_0 \left[ 1 + \frac{\lambda_0^2 D_0}{\nu_0^2} \frac{S_d}{[2\pi]^d} \left( \frac{6-d}{4d} \right) \left( \frac{e^{(4-d)r} - 1}{(4-d)\Lambda_0^{4-d}} \right) \right]. \quad (11)$$

The two point height-height correlation function corresponding to one-loop perturbative expansion can be written as

$$\langle h^<(\mathbf{k}, \omega) h^<(\mathbf{k}', \omega') \rangle = 2[D_0 + \Delta D] |G(\mathbf{k}, \omega)|^2 [2\pi]^{d+1} \delta^d(\mathbf{k} + \mathbf{k}') \delta(\omega + \omega') \quad (12)$$

where

$$\Delta D = \left( \frac{-\lambda_0}{2} \right)^2 (2D_0)^2 k^4 \int^> \frac{d^d q}{[2\pi]^d} [\mathbf{q} \cdot (\mathbf{k} - \mathbf{q})]^2 \int_{-\infty}^{\infty} \frac{d\Omega}{[2\pi]} |G_0^>(\hat{q})|^2 |G_0^>(\hat{k} - \hat{q})|^2 \quad (13)$$

which comes from the amputated part of the loop diagram shown in figure 1(b). The frequency and momentum integrations in equation 13 are carried out yielding

$$\Delta D = k^4 \left( \frac{K_d \lambda_0^2 D_0^2}{4\nu_0^3} \right) \left[ \frac{\Lambda_0^{d-8} - \Lambda^{d-8}(r)}{d-8} \right] \quad (14)$$

Since  $\Delta D$  goes like  $k^4$ , this correction to  $D_0$  is irrelevant in the large-scale and long-time limits. Hence

$$D^<(r) = D_0. \quad (15)$$

According to Lai and Das Sarma [23], the vertex ( $\lambda_0$ ) does not get any corrections from the RG transformation at one-loop order, consequently

$$\lambda^<(r) = \lambda_0. \quad (16)$$

## 2.2. Flow equations and Fixed point

We obtained the flow equations as differential equations with respect to variation of the parameter  $r$  from equations 11, 15 and 16 giving

$$\begin{aligned}\frac{d\nu}{dr} &= K_d \frac{\lambda_0^2 D_0 \Lambda^{d-4}(r)}{\nu^2(r)} \left( \frac{6-d}{4d} \right) \\ \frac{dD}{dr} &= 0 \\ \frac{d\lambda}{dr} &= 0\end{aligned}\tag{17}$$

where  $\Lambda(r) = \Lambda_0 e^{-r}$ . We define an effective coupling parameter

$$g(r) = K_d \frac{\lambda_0^2 D(r)}{\nu^3(r) \Lambda^{4-d}(r)}.\tag{18}$$

Using equations 17 and 18, we obtain the flow equation for the coupling constant

$$\frac{dg(r)}{dr} = a g(r) - b g^2(r)\tag{19}$$

where  $a = (4-d)$  and  $b = \frac{3(6-d)}{4d}$ . Integrating equation 19 over  $r$ , yields

$$g(r) = \frac{g_0 e^{ar}}{1 + \frac{b}{a} g_0 (e^{ar} - 1)},\tag{20}$$

where  $g(0) = g_0 = \frac{K_d \lambda_0^2 D_0}{\nu_0^3 \Lambda_0^{4-d}}$ . In the asymptotic limit of  $r$  ( $r \rightarrow \infty$ ), equation 20 approaches to  $r$  independent quantity

$$g^* = \frac{4d(4-d)}{3(6-d)}.\tag{21}$$

The fixed point, expressed by equation 21, is stable for  $d < 4$ , thereby the upper critical dimension of the VLDS equation is  $d_c = 4$  which agrees with Refs. [23, 24].

## 2.3. Renormalized Surface Diffusivity

Integrating the first flow equation in equation 17 using equation 19, we obtain

$$\nu(r) = \nu_0 \left[ 1 + \frac{b}{a} g_0 (e^{ar} - 1) \right]^{1/3}.\tag{22}$$

In the asymptotic limit of large  $r$ , equation 22 takes the form

$$\nu(r) = \nu_0 \left( \frac{b g_0}{a} e^{ar} \right)^{1/3},\tag{23}$$

and, in  $(1+1)$  dimensions, the above equation becomes

$$\nu(r) = \nu_0 \left( \frac{5 g_0}{4} \right)^{1/3} e^r.\tag{24}$$

Thus the corresponding renormalized surface diffusivity reads

$$\nu(k) = \nu_0 \left( \frac{5\lambda_0^2 D_0}{4\pi\nu_0^3} \right)^{1/3} k^{-1}, \quad (25)$$

in the large-scale long-time limits. The renormalized response function  $G(\mathbf{k}, \omega)$  and the dynamic exponent  $z$  is related through the expression

$$G^{-1}(\mathbf{k}, \omega) = [-i\omega + \nu(k)k^4] \propto k^z \xi \left( \frac{\omega}{k^z} \right). \quad (26)$$

The above equation indicates that  $\nu(k)k^4 \sim k^z$  implying dynamic exponent  $z = 3$  in  $d = 1$  dimension. The roughness exponent,  $\chi = 1$ , can be obtained from the scaling relation  $\chi + z = 4$ .

### 3. The Second Moment

Using the definition of  $n$ th moment of the height fluctuations expressed in equation 5, the second and third moments are obtained as

$$W_2 = \langle h^2(\mathbf{x}, t) \rangle - \langle h(\mathbf{x}, t) \rangle^2. \quad (27)$$

and

$$W_3 = \langle h^3(\mathbf{x}, t) \rangle - 3\langle h^2(\mathbf{x}, t) \rangle \langle h(\mathbf{x}, t) \rangle + 2\langle h(\mathbf{x}, t) \rangle^3, \quad (28)$$

respectively. Here  $h(\mathbf{x}, t)$  is the height fluctuations satisfying  $\langle h(\mathbf{x}, t) \rangle = 0$ , and consequently equation 27 and equation 28 become

$$W_2 = \langle h^2(\mathbf{x}, t) \rangle \quad (29)$$

and

$$W_3 = \langle h^3(\mathbf{x}, t) \rangle, \quad (30)$$

#### 3.1. Calculation of $W_2^{(1)}$

The perturbative expansion at one-loop order of the second moment yields

$$W_2 = \langle [h(\mathbf{x}, t)]^2 \rangle = W_2^{(1)} + W_2^{(2)} + W_2^{(3)}, \quad (31)$$

where  $W_2^{(1)}$  and  $W_2^{(2)}$  are non-zero contributions corresponding to  $O[\lambda_0^0]$  and  $O[\lambda_0^2]$  of the perturbation series. In Fourier space, the expression for  $W_2^{(1)}$  is written as

$$W_2^{(1)} = \int \frac{d^d k d\omega}{[2\pi]^{d+1}} \int \frac{d^d k' d\omega'}{[2\pi]^{d+1}} Q^{(0)}(\mathbf{k}, \omega; \mathbf{k}', \omega') e^{i(\mathbf{k}+\mathbf{k}') \cdot \mathbf{x}} e^{-i(\omega+\omega')t}. \quad (32)$$

The diagrammatic representation of  $W_2^{(1)}$  is shown in figure 1(a). We incorporate two point correlation (zeroth order), namely,  $Q^{(0)}(\mathbf{k}, \omega; \mathbf{k}', \omega') \equiv \langle h(\mathbf{k}, \omega) h(\mathbf{k}', \omega') \rangle = 2D_0 [2\pi]^{d+1} |G(\mathbf{k}, \omega)|^2 \delta^d(\mathbf{k} + \mathbf{k}') \delta(\omega + \omega')$  and carry out integration over  $k'$  yielding

$$W_2^{(1)} = 2D_0 \int \frac{d^d k}{[2\pi]^d} \int \frac{d\omega}{[2\pi]} |G(\mathbf{k}, \omega)|^2. \quad (33)$$

We use the functional form of  $\nu(k)$  from equation 25. Consequently performing the frequency integration and carrying out the momentum integration in (1+1) dimensions in equation 33, we obtain

$$W_2^{(1)} = \frac{1}{2\pi^{2/3}} \left( \frac{4D_0^2}{5\lambda_0^2} \right)^{1/3} \frac{1}{\mu^2} \quad (34)$$

where  $\mu$  is the lower limit of the momentum integration.

### 3.2. Calculation of $W_2^{(2)}$

The expression for  $W_2^{(2)}$  is expressed in momentum and frequency spaces as

$$W_2^{(2)} = \int \frac{d^d k d\omega}{[2\pi]^{d+1}} \int \frac{d^d k' d\omega'}{[2\pi]^{d+1}} Q^{(2)}(\mathbf{k}, \omega; \mathbf{k}', \omega') e^{i(\mathbf{k}+\mathbf{k}') \cdot \mathbf{x}} e^{-i(\omega+\omega')t}. \quad (35)$$

where  $Q^{(2)}(\mathbf{k}, \omega; \mathbf{k}', \omega') = [2\pi]^{d+1} L_2(\mathbf{k}, \omega) |G(\mathbf{k}, \omega)|^2 \delta^d(\mathbf{k}+\mathbf{k}') \delta(\omega+\omega')$ . Feynman diagram for  $W_2^{(2)}$  is given in figure 1(b). One-loop contribution to the second moment is given by

$$W_2^{(2)} = \int \frac{d^d k d\omega}{[2\pi]^{d+1}} G(\mathbf{k}, \omega) L_2(\mathbf{k}, \omega) G(-\mathbf{k}, -\omega) \quad (36)$$

where  $L_2$  [ $L_2 = k^4 l_2(\hat{k})$ ] corresponds to the amputated loop of figure 1(b) expressed in equation 13. We carry out the integrations over the internal frequencies and internal momenta in the shell  $\Lambda_0 e^{-r} \leq k \leq \Lambda_0$  and obtain

$$l_2^<(r) = \left( \frac{\lambda_0^2 D_0^2}{2\pi\nu_0^3} \right) \left[ \frac{\Lambda_0^{-7} - \Lambda^{-7}(r)}{-7} \right] \quad (37)$$

leading to the differential equation

$$\frac{dl_2}{dr} = \frac{\lambda_0^2 D_0^2}{2\pi\nu^3(r)\Lambda^7(r)}. \quad (38)$$

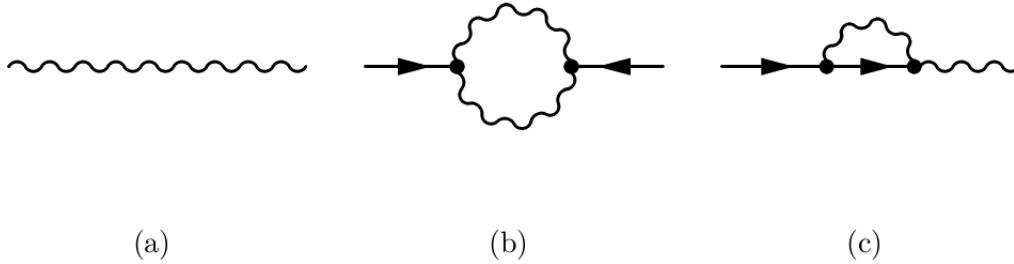


**Figure 1.** Feynman diagrams : (a)  $W_2^{(1)}$ , (b)  $W_2^{(2)}$  and (c)  $W_2^{(3)}$ . Responses are indicated by solid lines with arrow and correlation by a wiggly line.

The function  $\nu(r)$  being known from equation 24, the above differential equation is solved to obtain

$$l_2(r) = \left( \frac{D_0}{10\Lambda_0^4} \right) e^{4r} \quad (39)$$



in the asymptotic limit of large  $r$ . Identifying  $\Lambda_0 e^{-r} = k$ , we get

$$l_2(k, 0) = \frac{1}{10} D_0 k^{-4}. \quad (40)$$

The vertex of figure 1(b) contains  $k^4$  and consequently the loop contribution (without the external legs) becomes we define  $L_2(k, 0) = k^4 l_2(k, 0)$

$$L_2 = \frac{1}{10} D_0. \quad (41)$$

which is scale independent. Now substituting equation 41 in equation 36, we get

$$W_2^{(2)} = \int \frac{d^d k}{(2\pi)^d} \int \frac{d\omega}{[2\pi]} |G(\mathbf{k}, \omega)|^2 L_2 \quad (42)$$

Performing the frequency integration in equation 42, we obtain

$$W_2^{(2)} = \frac{1}{20\pi^{2/3}} \left( \frac{4D_0^2}{5\lambda_0^2} \right)^{1/3} \int_{\mu}^{\infty} dk k^{-3}. \quad (43)$$

We carry out the momentum integration in the above equation leading to

$$W_2^{(2)} = \frac{1}{40\pi^{2/3}} \left( \frac{4D_0^2}{5\lambda_0^2} \right)^{1/3} \frac{1}{\mu^2}. \quad (44)$$

Feynman diagram corresponding to  $W_2^{(3)}$  is shown in figure 1(a). The contribution to  $W_2^{(3)}$  vanishes in the large-scale limit. Adding the contributions  $W_2^{(1)}$  and  $W_2^{(2)}$  from equations 34 and 44, we obtain  $W_2$  as

$$W_2 = W_2^{(1)} + W_2^{(2)} = \frac{21}{40\pi^{2/3}} \left( \frac{4D_0^2}{5\lambda_0^2} \right)^{1/3} \frac{1}{\mu^2} \quad (45)$$

#### 4. The Third Moment and Skewness

The third moment of height fluctuations is expressed as

$$W_3 = \sum_{i=1}^8 W_3^{(i)} \quad (46)$$

where  $W_3^{(1)}$  and  $W_3^{(2)}$ , corresponding to Feynman diagrams Figs. 2(a) and 2(b) respectively, give non-zero contributions. The terms  $W_3^{(3)}$  and  $W_3^{(4)}$ , corresponding to figures 3(a) and 3(b), respectively, give equal magnitudes of logarithmic corrections with opposite signs and thus they cancel each other. The rest of the terms in equation 46, namely,  $W_3^{(5)}$ ,  $W_3^{(6)}$ ,  $W_3^{(7)}$  and  $W_3^{(8)}$ , are depicted in Figs. 4(a), 4(b), 4(c) and 4(d), respectively, which give zero contributions individually in the large-scale long-time limits.

#### 4.1. Calculation of $W_3^{(1)}$

In this subsection, we calculate Feynman diagram given in figure 2(a). The integral expression for  $W_3^{(1)}$  in the Fourier space is given by

$$W_3^{(1)} = \int \frac{d^d k_1 d\omega_1}{[2\pi]^{d+1}} \int \frac{d^d k_2 d\omega_2}{[2\pi]^{d+1}} \int \frac{d^d k_3 d\omega_3}{[2\pi]^{d+1}} \langle h(\mathbf{k}_1, \omega_1) h(\mathbf{k}_2, \omega_2) h(\mathbf{k}_3, \omega_3) \rangle e^{i(\mathbf{k}_1 + \mathbf{k}_2 + \mathbf{k}_3) \cdot \mathbf{x}} e^{-i(\omega_1 + \omega_2 + \omega_3)t}, \quad (47)$$

The third order height correlation appearing in equation 47 is expressed as

$$\langle h(\mathbf{k}_1, \omega_1) h(\mathbf{k}_2, \omega_2) h(\mathbf{k}_3, \omega_3) \rangle = G(\hat{k}_1) G(\hat{k}_2) G(\hat{k}_3) L_3^{(1)}(\hat{k}_1; \hat{k}_2; \hat{k}_3) \times [(2\pi)^{d+1} \delta^{d+1}(\hat{k}_1 + \hat{k}_2 + \hat{k}_3)] \quad (48)$$

where  $L_3^{(1)}(\hat{k}_1; \hat{k}_2; \hat{k}_3) = \mathbf{k}_1^2 \mathbf{k}_2^2 \mathbf{k}_3^2 l_3(\hat{k}_1; \hat{k}_2; \hat{k}_3)$  represents the renormalized amputated part of the loop diagram [figure 2(a)]. Substituting equation 48, in equation 47, we obtain

$$W_3^{(1)} = \int \frac{d^{d+1} \hat{k}_1}{[2\pi]^{d+1}} \int \frac{d^{d+1} \hat{k}_2}{[2\pi]^{d+1}} G(\hat{k}_1) G(\hat{k}_2) L_3^{(1)}(\hat{k}_1; \hat{k}_2) G(-\hat{k}_1 - \hat{k}_2) \quad (49)$$

The bare value of  $l_3^{(1,0)}(\hat{k}_1; \hat{k}_2)$  is given by

$$l_3^{(1,0)}(k_1, \omega_1; k_2, \omega_2) = 8 \left( \frac{-\lambda_0}{2} \right)^3 \int \frac{d^d q d\omega}{[2\pi]^{d+1}} [(\mathbf{q} - \mathbf{k}_1) \cdot (\mathbf{k}_2 + \mathbf{k}_1 - \mathbf{q})][\mathbf{q} \cdot (\mathbf{k}_1 - \mathbf{q})] \times [-\mathbf{q} \cdot (\mathbf{q} - \mathbf{k}_2 - \mathbf{k}_1)] Q_0(\hat{\mathbf{q}}) Q_0(\hat{\mathbf{k}}_1 - \hat{\mathbf{q}}) Q_0(\hat{\mathbf{k}}_1 + \hat{\mathbf{k}}_2 - \hat{\mathbf{q}})]. \quad (50)$$

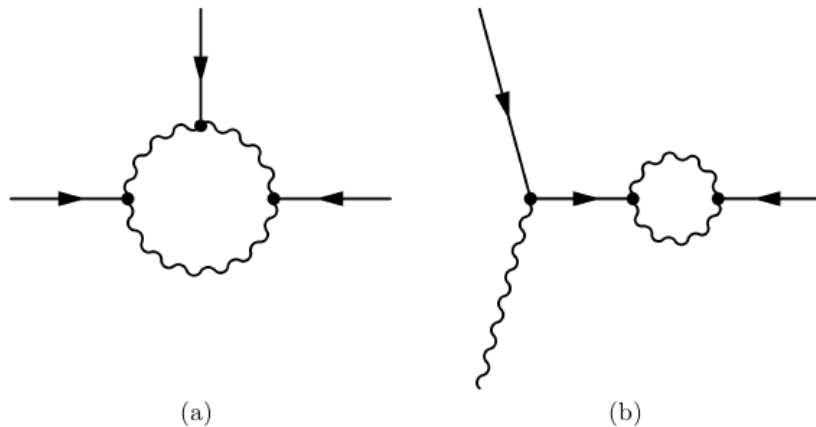


**Figure 2.** Feynman diagrams: (a)  $W_3^{(1)}$  and (b)  $W_3^{(2)}$ . These diagrams contribute to  $W_3$ .

where  $Q_0(\mathbf{q}) = 2D_0 [2\pi]^{d+1} G_0(\hat{q}) G_0(\hat{q}') \delta^{d+1}(\hat{q} + \hat{q}')$  are the correlations. Considering the external momenta and frequencies to be much smaller in magnitude than

internal momenta and frequencies, we carry out frequency convolution and momentum integrations yielding

$$l_3^{(1)<}(r) = \frac{3}{2} \left[ \frac{\lambda_0^3 D_0^3 K_d}{\nu_0^5 \Lambda_0^{14-d}} \right] \left[ \frac{e^{(14-d)r} - 1}{(14-d)} \right]. \quad (51)$$

The iterative nature of the shell elimination scheme yields

$$\frac{dl_3^{(1)}}{dr} = \frac{3}{2} \left[ \frac{\lambda_0^3 D_0^3 K_d}{\nu^5(r) \Lambda^{14-d}(r)} \right] \quad (52)$$

Solving this equation in the asymptotic limit of large  $r$  in  $d = 1$  dimension, we obtain

$$l_3^{(1)}(r) = \frac{3}{20} \lambda_0 D_0^2 \left( \frac{4\pi}{5\lambda_0^2 D_0} \right)^{2/3} \frac{1}{\Lambda^8(r)}. \quad (53)$$

$\Lambda_0 e^{-r}$  is identified as the external momenta, yielding

$$l_3^{(1)}(k_1, 0; k_2, 0) = \frac{3}{20} \lambda_0 D_0^2 \left( \frac{4\pi}{5\lambda_0^2 D_0} \right)^{2/3} k_1^{-4} k_2^{-4}. \quad (54)$$

So,  $L_3^{(1)}$  becomes

$$L_3^{(1)}(\mathbf{k}_1, \mathbf{k}_2) = \mathbf{k}_1^2 \mathbf{k}_2^2 \mathbf{k}_3^2 l_3^{(1)} \quad (55)$$

Now to find the wave vector and frequency dependence in equation 54 a form of scaling function is introduced by replacing  $k_i^{-2}$  by

$$k_i^{-2} f_d \left( \frac{\omega_i}{k_i^z} \right) = k_i^6 \nu^2(k_i) |G(\mathbf{k}_i, \omega_i)|^2 \quad (56)$$

where  $i = 1, 2$  and  $f(0) = 1$ . This expression is the same as  $k_i^{-2}$  for  $\omega_i = 0$ . Incorporating equation 56 in equation 54, we obtain

$$L_3^{(1)}(\hat{k}_1, \hat{k}_2) = \frac{3}{20} A k_1^4 k_2^4 |\mathbf{k}_1 + \mathbf{k}_2|^2 |G(\hat{k}_1)|^2 |G(\hat{k}_2)|^2 \quad (57)$$

with  $A = \lambda_0 D_0^2 \left( \frac{5\lambda_0^2 D_0}{4\pi} \right)^{2/3}$ . We substitute equation 57 in equation 49 yielding

$$W_3^{(1)} = \frac{3}{20} A \int \frac{d^2 \hat{k}_1}{[2\pi]^2} \int \frac{d^2 \hat{k}_2}{[2\pi]^2} k_1^4 k_2^4 |\mathbf{k}_1 + \mathbf{k}_2|^2 |G(\hat{k}_1)|^2 |G(\hat{k}_2)|^2 \\ \times [G(\hat{k}_1) G(\hat{k}_2) G(-\hat{k}_1 - \hat{k}_2)] \quad (58)$$

Carrying out the frequency integrations over  $\omega_1$  and  $\omega_2$ , we obtain

$$W_3^{(1)} = \left( \frac{3}{20} \right) \frac{A_1}{[2\pi]^2} \int_{-\infty}^{\infty} dk_1 \int_{-\infty}^{\infty} dk_2 F_1(k_1, k_2). \quad (59)$$

where

$$F_1(k_1, k_2) = \frac{3\sigma^2(k_1) + (\sigma(k_2) + \sigma(|k_1 + k_2|))(3\sigma(k_2) + \sigma(|k_1 + k_2|)) + 2\sigma(k_1)(7\sigma(k_2) + 2\sigma(|k_1 + k_2|))}{16\sigma^2(k_1)\sigma^2(k_2)(\sigma(k_1) + \sigma(k_2) + \sigma(|k_1 + k_2|))^3} \quad (60)$$

with  $\sigma(k_i) = k_i^3$  and  $A_1 = \frac{A (4\pi)^{5/3}}{(5\lambda_0^2 D_0)^{5/3}} = \left( \frac{4\pi D_0}{5\lambda_0} \right)$ . Now the integrations become

$$I_1(\mu) = \int_{\mu}^{\infty} dk_1 \int_{\mu}^{\infty} dk_2 F_1(k_1, k_2)$$

and

$$J_1(\mu) = \int_{\mu}^{\infty} dk_1 \int_{\mu}^{\infty} dk_1 F_1(-k_1, k_2).$$

Since these integrals are infrared divergent, we write them as

$$\begin{aligned} I_1(\mu) &= I_1^{(0)} \mu^{-3} \\ J_1(\mu) &= J_1^{(0)} \mu^{-3}. \end{aligned} \quad (61)$$

where  $I_1^{(0)}$  and  $J_1^{(0)}$  are dimensionless numerical constants. Carrying out numerical integrations, we obtain the values for the constants as

$$\begin{aligned} I_1^{(0)} &= \lim_{\mu \rightarrow 0^+} [\mu^3 I_1(\mu)] = 0.0148673 \\ J_1^{(0)} &= \lim_{\mu \rightarrow 0^+} [\mu^3 J_1(\mu)] = 0.0039435, \end{aligned} \quad (62)$$

Substituting equations 61 and 62 in equation 59, we obtain

$$\begin{aligned} W_3^{(1)} &= \frac{3}{100\pi} \left( \frac{D}{\lambda_0} \right) (2I_1^{(0)} + 2J_1^{(0)}) \frac{1}{\mu^3} \\ &= \frac{3}{50\pi} \left( \frac{D}{\lambda_0} \right) (0.018811) \frac{1}{\mu^3}. \end{aligned} \quad (63)$$

#### 4.2. Calculation of $W_3^{(2)}$

Feynman diagram for  $W_3^{(2)}$  is shown in figure 2(b). The integral expression for  $W_3^{(2)}$  is written as

$$\begin{aligned} W_3^{(2)} &= \int \frac{d^{d+1}\hat{k}}{[2\pi]^{d+1}} \int \frac{d^{d+1}\hat{k}'}{[2\pi]^{d+1}} \int \frac{d^{d+1}\hat{k}''}{[2\pi]^{d+1}} \int \frac{d^{d+1}\hat{q}}{[2\pi]^{d+1}} \int \frac{d^{d+1}\hat{p}}{[2\pi]^{d+1}} \int \frac{d^{d+1}\hat{Q}}{[2\pi]^{d+1}} \\ &\quad [k'^2 G(\hat{k}') k''^2 G(\hat{k}'') Q^2 G(\hat{Q})] [\mathbf{q} \cdot (\mathbf{k}' - \mathbf{q})] [\mathbf{Q} \cdot (\mathbf{k}'' - \mathbf{Q})] [\mathbf{p} \cdot (\mathbf{Q} - \mathbf{p})] \\ &\quad \times [\langle h(\hat{k}) h(\hat{q}) h(\hat{k}' - \hat{q}) h(\hat{k}'' - \hat{Q}) h(\hat{p}) h(\hat{Q} - \hat{p}) \rangle] \end{aligned} \quad (64)$$

The height correlation appearing in equation 64 is expressed as

$$\begin{aligned} \langle h(\hat{k}) h(\hat{q}) h(\hat{k}' - \hat{q}) h(\hat{k}'' - \hat{Q}) h(\hat{p}) h(\hat{Q} - \hat{p}) \rangle &= 24(2D_0)^3 [2\pi]^{3(d+1)} [|G_0(\hat{q})|^2] |G_0(\hat{k}' - \hat{q})|^2 \\ &\quad \times |G(\hat{k})|^2 [G(\hat{k}') k'^2] [G(-\hat{k} - \hat{k}') |\mathbf{k} + \mathbf{k}'|^2] [\mathbf{k}'^2 G(-\hat{k}')] \delta^{d+1}(\hat{k} + \hat{k}' + \hat{k}'') [\delta^{d+1}(\hat{p} + \hat{q})] \\ &\quad \times [\delta^{d+1}(\hat{Q} + \hat{k}')] \end{aligned} \quad (65)$$

Substituting the above form in equation 64, we obtain

$$\begin{aligned} W_3^{(2)} &= 12(\lambda_0 D_0) \int \frac{d^{d+1}\hat{k}}{[2\pi]^{d+1}} \int \frac{d^{d+1}\hat{k}'}{[2\pi]^{d+1}} |\mathbf{k} + \mathbf{k}'|^2 [\mathbf{k}' \cdot (-\mathbf{k})] |G(\hat{k}')|^2 |G(\hat{k})|^2 G(\hat{k} - \hat{k}') \\ &\quad L_3^{(2)}(\hat{k}') \end{aligned} \quad (66)$$

where  $L_3^{(2)}(\hat{k}') = k'^4 l_3^{(2)}(\hat{k}')$  and

$$l_3^{(2)}(\hat{k}') = 2(\lambda_0 D_0)^2 \int \frac{d^{d+1}q}{[2\pi]^{d+1}} [\mathbf{q} \cdot (\mathbf{q} - \mathbf{k}')]^2 [\mathbf{q} \cdot (\mathbf{k}' - \mathbf{q})] |G_0(\hat{k}' - \hat{q})|^2 |G_0(\hat{q})|^2 \quad (67)$$

We consider the external momenta and frequencies are much smaller in magnitude than internal momenta and frequencies and perform the frequency integration and momentum integration in the range  $\Lambda_0 e^{-r} \leq q \leq \Lambda_0$  leading

$$l_3^{(2)<}(r) = \frac{(\lambda_0 D_0)^2 K_d}{2\nu_0^3} \left[ \frac{\Lambda_0^{d-8} - \Lambda^{d-8}(r)}{(d-8)} \right]. \quad (68)$$

We construct a differential equation for  $l_3^{(2)}(r)$  by considering the iterative nature of the procedure

$$\frac{dl_3^{(2)}}{dr} = \frac{\lambda_0^2 D_0^2 K_d}{2\nu^3(r)} \Lambda^{d-8}(r) \quad (69)$$

Integrating over  $r$ , we obtain

$$l_3^{(2)}(r) = \frac{D_0}{10} \Lambda^{-4}(r) \quad (70)$$

in  $d = 1$  dimension. We identify  $\Lambda(r)$  as an external momentum and obtain

$$L_3^{(2)} = k'^4 l_3^{(2)}(k', 0) = D_0/10 \quad (71)$$

which is an scale independent quantity. We substitute equation 71 in equation 66 leading to

$$W_3^{(2)} = \frac{6}{5} (\lambda_0 D_0^2) \int \frac{d^2 \hat{k}}{[2\pi]^2} \int \frac{d^2 \hat{k}'}{[2\pi]^2} [-\mathbf{k}' \cdot \mathbf{k}] |\mathbf{k} + \mathbf{k}'|^2 |G(\hat{k}')|^2 |G(\hat{k})|^2 G(-\hat{k} - \hat{k}') \quad (72)$$

Carrying out the frequency integration, we obtain

$$W_3^{(2)} = -\frac{6\pi}{25} \left( \frac{D_0}{\lambda_0} \right) \int_{-\infty}^{\infty} \frac{dk}{[2\pi]} \int_{-\infty}^{\infty} \frac{dk'}{[2\pi]} F_2(k, k') \quad (73)$$

where

$$F_2(k, k') = \frac{(k'k)(k+k')^2}{|k|^3 |k'|^3 [|k|^3 + |k'|^3 + |k+k'|^3]} \quad (74)$$

We write

$$W_3^{(2)} = -\left( \frac{3}{50\pi} \right) \left( \frac{D_0}{\lambda_0} \right) [2(I_2(\mu) + J_2(\mu))] \quad (75)$$

where

$$I_2(\mu) = \int_{\mu}^{\infty} dk \int_{\mu}^{\infty} dk' F_2(k, k')$$

and

$$J_2(\mu) = \int_{\mu}^{\infty} dk \int_{\mu}^{\infty} dk' F_2(-k, k').$$

As before we write the integrals as

$$\begin{aligned} I_2(\mu) &= I_2^{(0)} \mu^{-3} \\ J_2(\mu) &= J_2^{(0)} \mu^{-3}. \end{aligned} \quad (76)$$

Numerical evaluations yield

$$\begin{aligned} I_2^{(0)} &= \lim_{\mu \rightarrow 0^+} [\mu^3 I_2(\mu)] = 0.154439 \\ J_2^{(0)} &= \lim_{\mu \rightarrow 0^+} [\mu^3 J_2(\mu)] = -0.020075, \end{aligned} \quad (77)$$

Substituting equations 77 and 76 in equation 75, we obtain

$$\begin{aligned} W_3^{(2)} &= \frac{3}{50\pi} (2I_2^{(0)} + 2J_2^{(0)}) \left( \frac{D}{\lambda_0} \right) \frac{1}{\mu^3} \\ &= -\frac{3}{50\pi} (0.268728) \left( \frac{D}{\lambda_0} \right) \frac{1}{\mu^3}. \end{aligned} \quad (78)$$

#### 4.3. Calculation of $W_3^{(3)}$

The integral expression for  $W_3^{(3)}$  can be written as

$$\begin{aligned} W_3^{(3)} &= \left( \frac{-\lambda_0}{2} \right)^3 \int \frac{d^{d+1}\hat{k}}{(2\pi)^{d+1}} \int \frac{d^{d+1}\hat{k}'}{(2\pi)^{d+1}} \int \frac{d^{d+1}\hat{p}}{(2\pi)^{d+1}} \int \frac{d^{d+1}\hat{q}}{(2\pi)^{d+1}} \int \frac{d^{d+1}\hat{q}'}{(2\pi)^{d+1}} \int \frac{d^{d+1}\hat{Q}}{(2\pi)^{d+1}} \\ &\quad \times [\mathbf{Q} \cdot (\mathbf{k}' - \mathbf{Q})][\mathbf{q}' \cdot (\mathbf{Q} - \mathbf{q}')] [\mathbf{q} \cdot (\mathbf{q}' - \mathbf{q})][G(\hat{k}')|k'|^2|Q^2||q'|^2 G_0(\hat{Q})G_0(\hat{q}')] \\ &\quad \times \langle h(\hat{p})h(\hat{k})h(\hat{k}' - \hat{Q})h(\hat{Q} - \hat{q}')h(\hat{q})h(\hat{q}' - \hat{q}) \rangle \end{aligned} \quad (79)$$

which is depicted in figure 3(a). The height correlation appearing in equation 79 is expressed as

$$\begin{aligned} \langle h(\hat{p})h(\hat{k})h(\hat{k}' - \hat{Q})h(\hat{Q} - \hat{q}')h(\hat{q})h(\hat{q}' - \hat{q}) \rangle &= 48(2D_0)^3 [2\pi]^{3(d+1)} |G_0(\hat{q}' + \hat{k})|^2 |G_0(\hat{p})|^2 \\ &\quad |G_0(\hat{k})|^2 \delta^{d+1}(\hat{Q} + \hat{p} - \hat{q}') \delta^{d+1}(\hat{q}' + \hat{k} - \hat{q}) \\ &\quad \delta^{d+1}(\hat{q}' - \hat{p} - \hat{k}') \end{aligned} \quad (80)$$

Substituting equation 80 in equation 79, we obtain

$$W_3^{(3)} = -48(\lambda_0 D_0)^3 \int \frac{d^{d+1}\hat{k}}{(2\pi)^{d+1}} \int \frac{d^{d+1}\hat{p}}{(2\pi)^{d+1}} |\mathbf{k} + \mathbf{p}|^2 |G(\hat{p})|^2 |G(\hat{k})|^2 |G(-\hat{k} - \hat{p})L_3(\hat{k}; \hat{p})| \quad (81)$$

where

$$\begin{aligned} l_3^{(3)}(\hat{k}; \hat{p}) &= \int \frac{d^{d+1}\hat{q}'}{(2\pi)^{d+1}} |\mathbf{q}' - \mathbf{p}|^2 |q'|^2 [\mathbf{q}' \cdot \mathbf{p}][(\mathbf{q}' - \mathbf{p}) \cdot (\mathbf{k} + \mathbf{q}')] [(\mathbf{q}' + \mathbf{k}) \cdot \mathbf{k}] G_0(\hat{q}') \\ &\quad G_0(\hat{q}' - \hat{p}) |G_0(\hat{q}' + \hat{k})|^2 \end{aligned} \quad (82)$$

Assuming the internal wave vector  $q'$  is much greater than external wave vectors  $p$  and  $k$ , we get

$$L_3^{(3)}(\mathbf{k}, 0; \mathbf{p}, 0) = - \int \frac{d^{d+1}q'}{[2\pi]^{d+1}} |q'|^6 [\mathbf{q}' \cdot \mathbf{p}][\mathbf{q}' \cdot \mathbf{k}] |G_0(\hat{q}')|^2 G_0^2(\hat{q}'). \quad (83)$$

Carrying out the frequency and momentum ( $\Lambda_0 e^{-r} \leq q' \leq \Lambda_0$ ) integration in  $d = 1$  dimension, we follow the same procedure as in Sec. 4.1 and obtain

$$L_3^{(3)}(p, 0; k, 0) = -\frac{pk}{10\lambda_0^2 D_0} \ln(\Lambda_0/k). \quad (84)$$

We substitute equation 84 in equation 81 and obtain

$$W_3^{(3)} = \frac{24}{5} (\lambda_0 D_0^2) I_3 \quad (85)$$

where

$$I_3 = \int \frac{dk d\omega_1}{[2\pi]^2} \int \frac{dp d\omega_2}{[2\pi]^2} [k p] ([k+p])^2 |G(\hat{k})|^2 |G(\hat{p})|^2 G(-\hat{k}-\hat{p}) \ln(\Lambda_0/k) \quad (86)$$

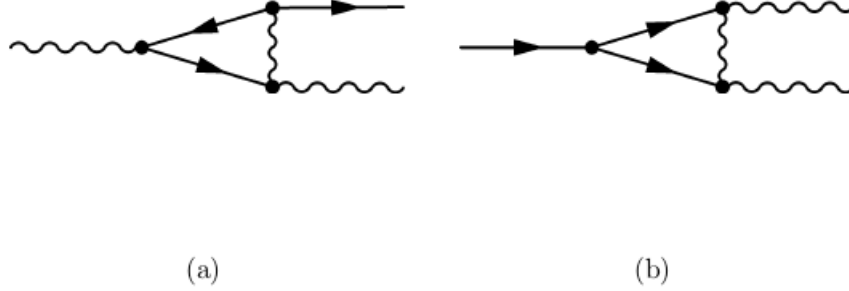


**Figure 3.** Feynman diagrams: (a)  $W_3^{(3)}$  and (b)  $W_3^{(4)}$ . These diagrams yield logarithmic corrections same in magnitude with opposite signs.

#### 4.4. Calculation of $W_3^{(4)}$

We express  $W_3^{(4)}$  in momentum and frequency spaces as

$$\begin{aligned} W_3^{(4)} = & \left( \frac{-\lambda_0}{2} \right)^3 \int \frac{d^{d+1}\hat{k}}{[2\pi]^{d+1}} \int \frac{d^{d+1}\hat{k}'}{[2\pi]^{d+1}} \int \frac{d^{d+1}\hat{p}}{[2\pi]^{d+1}} \int \frac{d^{d+1}\hat{q}}{[2\pi]^{d+1}} \int \frac{d^{d+1}\hat{q}'}{[2\pi]^{d+1}} \int \frac{d^{d+1}\hat{Q}}{[2\pi]^{d+1}} \\ & \times [\mathbf{q} \cdot (\mathbf{k}' - \mathbf{Q} - \mathbf{q})][\mathbf{Q} \cdot (\mathbf{k}' - \mathbf{Q})][\mathbf{q}' \cdot (\mathbf{Q} - \mathbf{q}')] |\mathbf{k}' - \mathbf{Q}|^2 |Q|^2 |k'|^2 G(\hat{Q}) G(\hat{k}') \\ & \times G(\hat{k}' - \hat{Q}) [\langle h(\hat{p}) h(\hat{k}) h(\hat{q}) h(\hat{q}') h(\hat{k}' - \hat{Q} - \hat{q}) h(\hat{Q} - \hat{q}') \rangle] \end{aligned} \quad (87)$$

and the corresponding Feynman diagram is depicted in figure 3(b). Height correlation in equation 87 is written as

$$\begin{aligned} \langle h(\hat{p}) h(\hat{k}) h(\hat{q}) h(\hat{q}') h(\hat{k}' - \hat{Q} - \hat{q}) h(\hat{Q} - \hat{q}') \rangle = & 24(2D_0)^3 [2\pi]^{3(d+1)} |G_0(\hat{k} + \hat{Q})|^2 |G_0(\hat{p})|^2 \\ & |G_0(\hat{k})|^2 \delta^{d+1}(\hat{q} + \hat{k} + \hat{Q}) \delta^{d+1}(\hat{Q} + \hat{q}' - \hat{k}) \\ & \delta^{d+1}(\hat{k} + \hat{k}' + \hat{p}). \end{aligned} \quad (88)$$

We substitute equation 88 in equation 87 and obtain

$$W_3^{(4)} = -24(\lambda_0 D_0)^3 \int \frac{d^{d+1}\hat{k}}{[2\pi]^{d+1}} \int \frac{d^{d+1}\hat{p}}{[2\pi]^{d+1}} |\mathbf{k} + \mathbf{p}|^2 |G(\hat{p})|^2 |G(\hat{k})|^2 |G(\hat{k} - \hat{p})| L_3^{(4)}(\hat{p}; \hat{k}) \quad (89)$$

where

$$l_3^{(4)}(\hat{p}; \hat{k}) = \int \frac{d^{d+1}\hat{Q}}{[2\pi]^{d+1}} [\mathbf{Q} \cdot (-\mathbf{k} - \mathbf{p} - \mathbf{Q})][(-\mathbf{k} - \mathbf{Q}) \cdot -\mathbf{p}][(\mathbf{k} + \mathbf{Q}) \cdot -\mathbf{k}] |\mathbf{k} + \mathbf{p} + \mathbf{Q}|^2 |Q|^2 G_0(\hat{Q}) G(-\hat{k} - \hat{p} - \hat{Q}) |G(\hat{k} + \hat{Q})|^2 \quad (90)$$

Considering external momenta and frequencies ( $\hat{p}$  and  $\hat{k}$ ) are much smaller than the internal momenta and frequency ( $\hat{Q}$ ), we obtain

$$l_3^{(4)}(\mathbf{p}, 0; \mathbf{k}, 0) = \int \frac{d^{d+1}\hat{Q}}{[2\pi]^{d+1}} [\mathbf{Q} \cdot \mathbf{k}] [\mathbf{Q} \cdot \mathbf{p}] |Q|^6 G_0(\hat{Q}) G(-\hat{k} - \hat{p} - \hat{Q}) |G(\hat{Q})|^2 \quad (91)$$

Performing the frequency integration and working out the momentum integration in the high-momentum shell  $\Lambda_0 e^{-r} \leq Q \leq \Lambda_0$ , we follow the same procedure as in Sec. 4.1 and 4.2 and obtain

$$l_3^{(4)}(p, 0; k, 0) = -\frac{p k}{5\lambda_0^2 D_0} \ln(\Lambda_0/k) \quad (92)$$

in  $d = 1$  dimension. We substitute equation 92 in equation 88 and get

$$W_3^{(4)} = -\frac{24}{5} (\lambda_0 D_0^2) I_4 \quad (93)$$

where

$$I_4 = \int \frac{dk d\omega_1}{[2\pi]^2} \int \frac{dp d\omega_2}{[2\pi]^2} [k p] ([k+p])^2 |G(\hat{k})|^2 |G(\hat{p})|^2 |G(-\hat{k} - \hat{p})| \ln(\Lambda_0/k). \quad (94)$$

It is seen that the integral form of  $I_3$  and  $I_4$ , expressed in equations 86 and 94, respectively, are identical. Hence the logarithmic contributions  $W_3^{(3)}$  and  $W_3^{(4)}$ , obtained in equations 85 and 93, respectively, are same in magnitude and opposite in signs. Thus, they cancel each other exactly and effectively do not contribute to  $W_3$ .

#### 4.5. Calculation of $W_3^{(5)}$

The expression for  $W_3^{(5)}$  in momentum and frequency space is given by

$$W_3^{(5)} = \left(\frac{-\lambda_0}{2}\right)^3 \int \frac{d^{d+1}\hat{k}}{[2\pi]^{d+1}} \int \frac{d^{d+1}\hat{k}'}{[2\pi]^{d+1}} \int \frac{d^{d+1}\hat{p}}{[2\pi]^{d+1}} \int \frac{d^{d+1}\hat{q}}{[2\pi]^{d+1}} \int \frac{d^{d+1}\hat{q}'}{[2\pi]^{d+1}} \int \frac{d^{d+1}\hat{Q}}{[2\pi]^{d+1}} [\mathbf{Q} \cdot (\mathbf{k}' - \mathbf{Q})][\mathbf{q} \cdot (\mathbf{p} - \mathbf{q})][\mathbf{q}' \cdot (\mathbf{Q} - \mathbf{q}')] |k'|^2 |p|^2 |Q|^2 G(\hat{k}') G(\hat{p}) G(\hat{Q}) \langle h(\hat{k}' - \hat{Q}) h(\hat{q}') h(\hat{Q} - \hat{q}') h(\hat{q}) h(\hat{p} - \hat{q}) h(\hat{k}') \rangle \quad (95)$$



Feynman diagram corresponding to  $W_3^{(5)}$  is shown in figure 4(a). We express the height correlation appearing in equation 95 as

$$\begin{aligned} \langle h(\hat{k}' - \hat{Q})h(\hat{q}')h(\hat{Q} - \hat{q}')h(\hat{q})h(\hat{p} - \hat{q})h(\hat{k}) \rangle &= 48(2D_0)^3 [2\pi]^{3(d+1)} G(\hat{p} + \hat{k}')G(\hat{k})|G(\hat{k}')|^2 \\ &\quad |G_0(\hat{k}' - \hat{Q})|^2 \delta^{d+1}(\hat{k}' + \hat{q}) \delta^{d+1}(\hat{k}' - \hat{q}') \\ &\quad \delta^{d+1}(\hat{k} + \hat{p} + \hat{k}'). \end{aligned} \quad (96)$$

Substituting equation 96 in equation 95, we obtain

$$\begin{aligned} W_3^{(5)} &= 48(2D_0)^2 \left( \frac{-\lambda_0}{2} \right)^3 \int \frac{d^{d+1}\hat{k}}{[2\pi]^{d+1}} \int \frac{d^{d+1}\hat{p}}{[2\pi]^{d+1}} |\mathbf{k} + \mathbf{p}|^2 |p|^2 G(-\hat{k} - \hat{p})G(\hat{p})G(\hat{k}) \\ &\quad |G(\hat{k} + \hat{p})|^2 [(\mathbf{k} + \mathbf{p}) \cdot \mathbf{k}] L_3^{(5)}(\hat{k} + \hat{p}) \end{aligned} \quad (97)$$

where

$$\begin{aligned} L_3^{(5)}(\hat{k} + \hat{p}) &= (2D_0) \int \frac{d^{d+1}\hat{Q}}{[2\pi]^{d+1}} [\mathbf{Q} \cdot (\mathbf{Q} + \mathbf{k} + \mathbf{p})][(\mathbf{Q} - \mathbf{k} - \mathbf{p}) \cdot (\mathbf{k} + \mathbf{p})] |Q|^2 G_0(\hat{Q}) \\ &\quad |G_0(\hat{k} + \hat{p} + \hat{Q})|^2 \end{aligned} \quad (98)$$

Considering internal momenta are much larger than the external momenta, we obtain

$$L_3^{(5)}(\hat{k} + \hat{p}) = -(2D_0) \int \frac{d^{d+1}\hat{Q}}{[2\pi]^{d+1}} |Q|^4 [\mathbf{Q} \cdot (\mathbf{k} + \mathbf{p})] G_0(\hat{Q}) |G_0(\hat{k} + \hat{p} + \hat{Q})|^2 \quad (99)$$

We perform the frequency integration and obtain

$$L_3^{(5)}(k + p) = -\frac{D_0}{4\nu_0^2} (k + p) \int_{-\infty}^{\infty} \frac{dQ}{[2\pi]} \frac{Q}{|Q|^4} = 0 \quad (100)$$

in  $d = 1$  dimension. Hence,  $W_3^{(5)}$  yields zero contribution. Similarly other terms such as  $W_3^{(6)}$ ,  $W_3^{(7)}$  and  $W_3^{(8)}$ , shown in Figs. 4(b), 4(c) and 4(d), respectively, give vanishing contributions individually.

#### 4.6. Skewness in One dimension

Adding all the terms on the right hand side of equation 46, we observe that the effective contribution to  $W_3$  comes from  $W_3^{(1)}$  and  $W_3^{(2)}$ , given in equations 45 and 101, yielding

$$W_3 = W_3^{(1)} + W_3^{(2)} = -\frac{3}{50\pi} [0.249917] \left( \frac{D_0}{\lambda_0} \right) \frac{1}{\mu^3}. \quad (101)$$

Hence, we calculate the skewness employing the definition given in equation 6 wherein we substitute the calculated values for  $W_2$  and  $W_3$  from equations 45 and 101. Thus we obtain

$$S = \frac{W_3}{W_2^{3/2}} = -0.044072 \quad (102)$$

which is independent of the model parameters  $(\lambda_0 \nu_0 D_0)$  and the momentum cutoffs  $(\mu_0, \Lambda_0)$ .

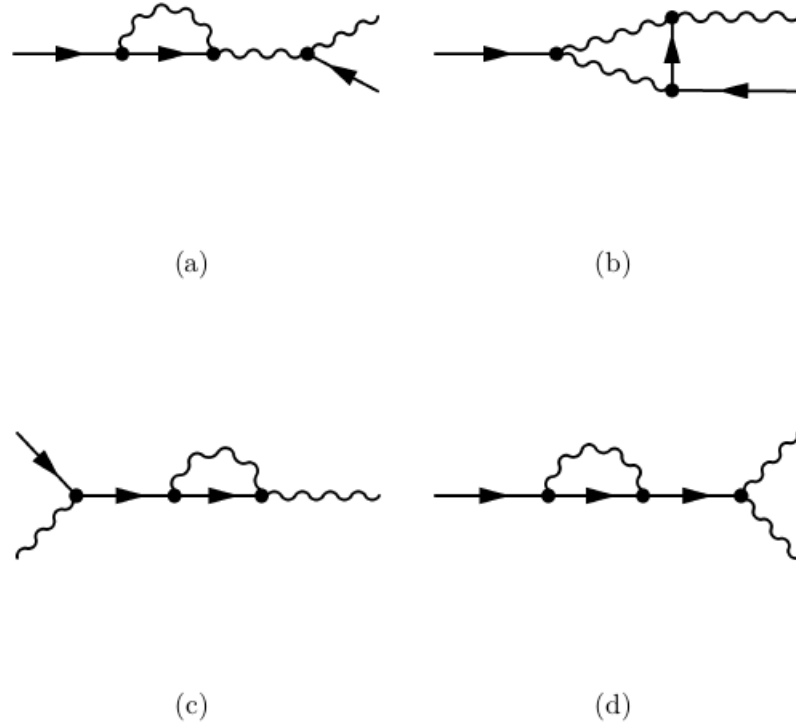


**Figure 4.** Feynman diagrams: (a)  $W_3^{(5)}$ , (b)  $W_3^{(6)}$ , (c)  $W_3^{(7)}$  and (d)  $W_3^{(8)}$ . These diagrams yield zero contributions individually.

## 5. Discussion and Conclusion

In this paper, we considered the conserved stochastic growth of a surface due to particle deposition on a flat substrate and we find the statistical properties of the surface in the large-scale long-time limits. The corresponding dynamics is represented by the VLDS equation driven by a stochastic Gaussian white noise. We followed an RG scheme without rescaling akin to Yakhot and Orszag [38, 39].

This RG scheme differs from the conventional dynamical RG scheme of Ma and Mazenko [43], Forster *et al.* [42], and Medina *et al.* [10] in the sense that the renormalized quantity are not rescaled and their flow equation are directly worked out. Thus, we obtained the renormalized diffusivity  $\nu(r)$  at large  $r$  and the roughness exponent  $\chi = 1$ . This is consistent with the previous RG results obtained by Lai and Das Sarma [23].

Subsequently, we calculate the skewness of height fluctuations of the VLDS equation. A similar scheme was employed earlier for the calculation of skewness [40] and kurtosis [41] in the case of non-conserved interface growth governed by the (1 + 1)-dimensional KPZ equation. The amputated parts of the connected loop diagrams, namely,  $l_2$ ,  $l_3^{(1)}$ ,  $l_3^{(2)}$ ,  $l_3^{(3)}$ ,  $l_3^{(4)}$  etc., for the second and third moments as shown in Figs. 1(b), 2(a), 2(b), 3(a), 3(b) etc., respectively, are renormalized by means of scale elimination and by constructing differential equations representing how these renormalized quantities flow with respect to the RG decimation scheme. The solutions

to the differential equations immediately yield their renormalized values. Employing this RG scheme, we directly find the renormalized expressions for these loop integrals which are indispensable for the calculation of moments. These renormalized amputated parts of the loops are used in conjunction with the external legs to numerically evaluate the integrals for the second and third moments.

Our approach subsumes calculations of  $W_2$  and  $W_3$  in the large scale limit  $k \rightarrow 0$  and consequently expects the statistical properties of the growth process at large scales. It is to be noted that these moments are independent of the upper cutoff  $\Lambda_0$  and functions of lower cutoff  $\mu$  which may be identified with the inverse of the substrate size  $L$ . These moments are also observed to follow the expected scaling  $W_n \sim L^{n\chi}$ . The value for the skewness is immediately obtained from these calculated values which is found to be independent of the model parameters  $(\lambda_0, D_0, \nu_0)$  and the UV and IR cutoffs  $(\Lambda_0, \mu)$ , suggesting its universality.

It is interesting to note that we obtained the skewness value which is a negative number. This is consistent with the numerical prediction of Das Sarma *et al.* [37] who obtained  $S = -0.1 \pm 0.15$  in the steady state and suggested that the skewness value is likely to be negative, although they did not exclude a zero or slightly positive value. The large error bar that they obtained is probably due to a dominant role of fluctuations in their numerical model. We observe that our value of  $S = -0.0441$  is consistent with their prediction. Moreover our calculated value asserts that the probability distribution function is negatively skewed.

### Acknowledgements

T.S. is thankful to the Ministry of Human Resource Development (MHRD), Government of India, for financial support through a scholarship.

### References

- [1] Barabási A-L and Stanley H E 1995 *Fractal Concepts in Surface Growth* (Cambridge: Cambridge University Press)
- [2] Krug J 1997 *Adv. Phys.* **46** 139
- [3] Halpin-Healy T and Zhang Y-C 1995 *Phys. Rep.* **254** 215
- [4] Meakin P 1993 *Phys. Rep.* **235** 189
- [5] Family F and Vicsek T 1985 *J. Phys. A: Math. Gen.* **18** L75
- [6] F. Family, *Physica A* **168**, 561 (1990).
- [7] I.V.Markov, *Crystal Growth for Beginners: Fundamentals of Nucleation, Crystal Growth and Epitaxy, 2nd ed.*, (World Scientific, Singapore, 2003).
- [8] D. Wilkinson and S. Edwards, **381**, 17 (1982).
- [9] Kardar M, Parisi G, and Zhang Y-C 1986 *Phys. Rev. Lett.* **56** 889
- [10] Medina E, Hwa T, Kardar M, and Zhang Y-C 1989 *Phys. Rev. A* **39**, 3053
- [11] Plischke M and Rácz Z 1985 *Phys. Rev. A* **32** 3825
- [12] Meakin P, Ramanlal P, Sander L M, and Ball R C 1986 *Phys. Rev. A* **34** 5091
- [13] Siegert M and Plischke M 1992 *Phys. Rev. Lett.* **68** 2035
- [14] Plischke M, Rácz Z, and Liu D 1987 *Phys. Rev. B* **35**, 3485
- [15] Yan H 1992 *Phys. Rev. Lett.* **68**, 3048

- [16] Reis F D A A 2004 *Phys. Rev. E* **70**, 031607
- [17] Villain J 1991 *J. Phys. I* **1** 19
- [18] Mullins W W 1959 *J. Appl. Phys.* **30**, 333
- [19] Wolf D E and Villain J 1990 *Europhys. Lett.* **13**, 389
- [20] Das Sarma S and Tamborenea P 1991 *Phys. Rev. Lett.* **66**, 325
- [21] Krug J 1994 *Phys. Rev. Lett.* **72**, 2907
- [22] Sun T, Guo H, and Grant M 1989 *Phys. Rev. A* **40**, 6763
- [23] Lai Z W and Das Sarma S 1991 *Phys. Rev. Lett.* **66**, 2348
- [24] Tang L H and Nattermann T 1991 *Phys. Rev. Lett.* **66**, 2899
- [25] Janssen H K 1997 *Phys. Rev. Lett.* **78**, 1082
- [26] Yook S H, Kim J M, and Kim Y 1997, *Phys. Rev. E* **56**, 4085
- [27] Yook S H, Lee C K, and Kim Y 1998 *Phys. Rev. E* **58**, 5150
- [28] Katzav E 2002 *Phys. Rev. E* **65**, 032103
- [29] Marsili M, Maritan A, Toigo F, and Banavar J R 1996 *Rev. Mod. Phys.* **68**, 963
- [30] Vvedensky D D, Zangwill A, Luse C N, and Wilby M R 1993 *Phys. Rev. E* **48**, 852
- [31] M. Předota and Kotrla M 1996 *Phys. Rev. E* **54**, 3933
- [32] Huang Z F and Gu B L 1996 *Phys. Rev. E* **54**, 5935
- [33] Huang Z F and Gu B L 1998 *Phys. Rev. E* **57**, 4480
- [34] Wilby M R, Vvedensky D D, and Zangwill A 1992 *Phys. Rev. B* **46**, 12896
- [35] Kim Y, Park D K, and Kim J M 1994 *J. Phys. A* **27**, L553
- [36] Kim Y and Kim J M 1997 *Phys. Rev. E* **55**, 3977
- [37] Das Sarma S, Lanczycki C J, Kotlyar R and Ghaisas S V 1996 *Phys. Rev. E* **53** 359
- [38] Yakhot V and Orszag S, *J. Sci. Comput.* **1**, 3 (1986).
- [39] Yakhot V and Orszag S A 1986 *Phys. Rev. Lett.* **57**, 1722
- [40] Singha T and Nandy M K 2014 *Phys. Rev. E* **90** 062402
- [41] Singha T and Nandy M K 2015 *J. Stat. Mech.: Theory and Exp.* **P05020**
- [42] Forster D, Nelson D R, and Stephen M J 1977 *Phys. Rev. A* **16**, 732
- [43] Ma S K and Mazenko G F 1975 *Phys. Rev. B* **11**, 4077